

# INTERNATIONAL SOCIETY FOR SOIL MECHANICS AND GEOTECHNICAL ENGINEERING



*This paper was downloaded from the Online Library of the International Society for Soil Mechanics and Geotechnical Engineering (ISSMGE). The library is available here:*

<https://www.issmge.org/publications/online-library>

*This is an open-access database that archives thousands of papers published under the Auspices of the ISSMGE and maintained by the Innovation and Development Committee of ISSMGE.*

# Irrecoverable Three-Dimensional Stress-Strain Relationship for Christie's Sand

by

J. W. PAPPIN, B.E.(Hons), Grad.I.E.Aust.

Experimental Officer, Division of Applied Geomechanics, CSIRO; formerly Graduate Student, University of Adelaide

**SUMMARY.** A sand at a constant initial void ratio was subjected to a series of reloading tests under varying stress conditions in a hollow cylinder apparatus, and elastic (recoverable) and plastic (irrecoverable) strains were identified and measured. The elastic response was satisfactorily expressed using stress dependent Young's modulus and Poisson's ratio. The plastic behaviour was analysed using elastic theory with classical plasticity theory, the three basic components of which (viz. the work-hardening law, the yield surface and plastic potential) were formulated and combined to obtain a realistic elasto-plastic mathematical model. It is shown that this method is viable and the variables can be determined from the normal triaxial test. Some valuable insights into the real behaviour of the soil were also discovered in this work.

## NOTATION

$\sigma_a$	= axial stress (compressive, positive)	$P_o$	= cell pressure
$\sigma_r$	= radial stress (compressive, positive)	$\epsilon_p^p$	= hydrostatic plastic strain
$\sigma_\theta$	= tangential stress (compressive, positive)	$\epsilon_q^p$	= deviatoric plastic strain
$\epsilon_a, \epsilon_r, \epsilon_\theta$	= corresponding strain (compressive, positive)	$\epsilon_a^p$	= plastic axial strain
$\sigma_q$	= deviatoric stress	$\phi$	= Mohr-Coulomb failure angle
$\sigma_q = \frac{1}{\sqrt{3}} [(\sigma_1 - \sigma_2)^2 + (\sigma_2 - \sigma_3)^2 + (\sigma_3 - \sigma_1)^2]^{1/2}$		$\lambda$	= non-negative parameter
$\sigma_p$	= hydrostatic stress $\sigma_p = \frac{\sigma_1 + \sigma_2 + \sigma_3}{\sqrt{3}}$	$K$	= gradient of plastic potential
$v$	= volumetric strain = $\epsilon_a + \epsilon_r + \epsilon_\theta$	$\sigma_{ij}$	= component of stress tensor
$v_p$	= plastic volumetric strain	$\epsilon_{ij}$	= component of strain tensor
$P_i$	= bore pressure	$g(\sigma_{ij})$	= plastic potential function

## 1 INTRODUCTION

A consideration of soil-structure interaction, although desirable, is usually neglected in present day design for lack of information on how soil behaves as a structural material. This paper demonstrates that routine laboratory testing can yield a realistic three-dimensional stress-strain relationship for a sand in a form compatible with current design techniques available on computer.

A hollow cylinder apparatus was used to test the material as it can apply three independent stresses to the sample. The other most commonly used three-dimensional test is the cuboidal test which suffers from stress concentrations due to corner effects (Ref. 1). If lubricated end platens are used, no significant stress concentrations occur. A disadvantage of the hollow cylinder test is that, if cell and pore pressures differ, the stress and strain states through the sample wall can only be calculated using an assumed stress-strain law; therefore this test can be used as a three-dimensional check on a mathematical model by comparing the predicted and experimental boundary stresses and strains.

It has been observed (Ref. 2, 3) that sands exhibit an elastic work-hardening plastic behaviour, i.e. under cyclic loading below a preloaded value the material is perfectly elastic yet upon loading above this maximum the sample behaves as if it were subjected to virgin loading (i.e. a combination of elastic

and plastic responses). This implies that the elastic and plastic strains are independent and can be measured separately. Hence if the elastic and plastic components of strain are analysed individually (Ref. 4), using elasticity and plasticity theories respectively, the behaviour of the material can be completely defined.

The elastic behaviour was adequately defined by the basic isotropic elastic theory using stress-dependent values of Young's modulus and Poisson's ratio. Young's modulus is found to be directly proportional to the hydrostatic stress and Poisson's ratio directly proportional to the deviatoric stress.

The classical plasticity theory prescribed by Hill (Ref. 5) and later by Poorooshab (Ref. 6) was chosen to express the plastic behaviour as the material work-hardens up to failure conditions (Ref. 7). The three independent basic components of this theory are:

- the work-hardening law,
- the yield surface, and
- the plastic potential flow rule.

### (a) The Work-Hardening Law

A material work-hardens when energy is required from an external source for it to suffer a plastic deformation. Sand exhibits this type of behaviour until failure. As the state of a soil element is uniquely defined by a stress-void ratio space, the

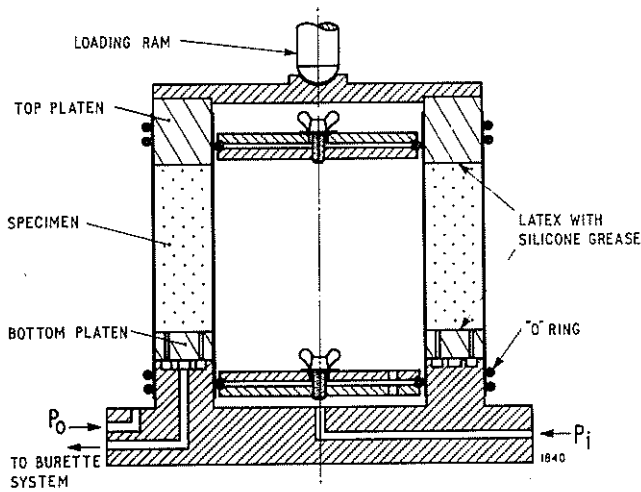


Fig. 1 Cross section of hollow cylinder

void ratio-stress relationship can be used as a work-hardening property. A failure criterion must also be determined to define the limits of stress space within which this law can exist.

### (b) Yield Surface

A yield surface defines the boundary of the stress region within which changes in stress cause no plastic deformation. This boundary is constantly changing during work-hardening and is unique at any stress state to which the material may be subjected.

### (c) Plastic Potential

The plastic potential is a surface in stress space that is everywhere perpendicular to the direction of the plastic strain increment vector. The hypothesis is made that the plastic potential is a scalar function of stress  $g(\sigma_{ij})$  from which the components of the plastic strain increments  $d\epsilon_{ij}^p$  may be found by partially differentiating  $g(\sigma_{ij})$  with respect to  $\sigma_{ij}$

$$\text{i.e. } d\epsilon_{ij}^p = \frac{\lambda dg(\sigma_{ij})}{d\sigma_{ij}} \quad (1)$$

where  $\lambda$  is a non-negative parameter.

If the principal plastic strain increment vectors are plotted on the same axis as the respective principal stresses the plastic potential surfaces can be geometrically determined.

By using a three-dimensional testing apparatus, these three basic components can be formulated and applied to the hollow cylinder problem. It is subsequently shown that this could also be achieved with a conventional triaxial test.

## 2 MATERIALS AND APPARATUS

The material testing was a worked, oven-dried, sub-rounded quartzitic sand, obtained from a site fifty kilometers south of Adelaide (Christie's Sand). It was artificially graded to the limits  $0.42 \text{ mm} < d < 1.20 \text{ mm}$  with 50% finer than  $0.65 \text{ mm}$ . The maximum and minimum void ratios were 0.89 and 0.60 respectively.

The hollow cylinder apparatus tested specimens of outer diameter 152 mm, inner diameter 102 mm and height approximately 140 mm. A cross-section is shown in Fig. 1. The whole apparatus fitted inside a conventional triaxial cell. The main feature of this device is that the cell pressure ( $P_o$ ), the bore pressure ( $P_i$ ) and the vertical load can all be independently applied and measured. The volume changes of the bore and cell were measured by the amount of water flowing in and out of each. These measurements were checked against a burette connected

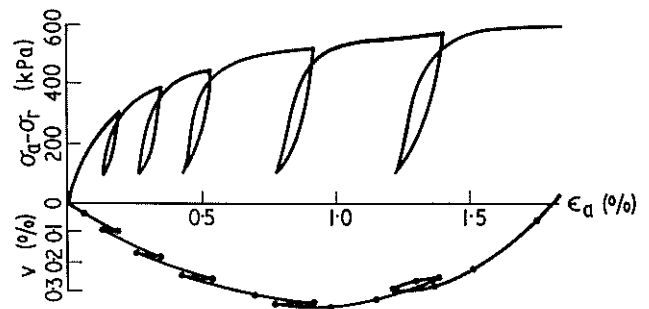


Fig. 2 Typical Series A test results

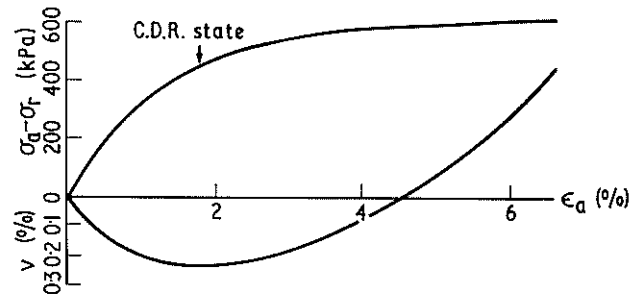


Fig. 3 Typical Series B test results

to the sample interior and good agreement was observed once membrane penetration effects etc. were taken into account. "Frictionless" end platens were used at the top and bottom of the samples. The dry sand was poured from a constant height and compacted to a void ratio  $0.74 \pm 0.01$  by ramming with a wooden rod. Throughout all tests the samples were dry and drained to atmospheric pressure.

## 3 TESTING PROGRAMME AND RESULTS

During testing the samples were statically loaded by controlled increments of axial force, and cell and bore pressure. The volume changes and vertical displacement were read after constant values were reached. Two series of tests were performed.

**Test Series A:** The sand was subjected to constant equal cell and bore pressures ( $P_i = P_o$ ) followed by axial (vertical) cyclic reloading up to failure. Eight tests were performed each at different values of equal cell and bore pressures. A typical test result is shown in Fig. 2; the failure point is not shown as it occurs at a much larger strain (about 8%). The elastic component of strain can be readily identified from these tests. It can be seen that at low shear stress values the elastic response is significant but at higher values the plastic response has much greater influence.

**Test Series B:** Fifteen tests were performed in this series. The sand was initially subjected to an equal cell and bore consolidation stress and then either the internal (13 tests conducted by Mitchell, Ref. 8) pressure or the external (2 tests) pressure was increased to a predetermined value. Then the axial load was applied incrementally (see Fig. 3 for a typical test result). The stress condition induced is  $\sigma_a > \sigma_r > \sigma_\theta$  for  $P_i > P_o$  and  $\sigma_a > \sigma_\theta > \sigma_r$  for  $P_o > P_i$ .

For Series A tests with the cell and bore pressures being equal, static equilibrium and strain compatibility considerations mean that the stresses and strains are known and constant throughout the sample and that the horizontal components are equal (i.e.  $\epsilon_r = \epsilon_\theta$ ,  $\sigma_r = \sigma_\theta$ ). This means that accurate measurements could be confidently made. For Series B tests the stress and strain distribution through the sample wall thickness are governed by the

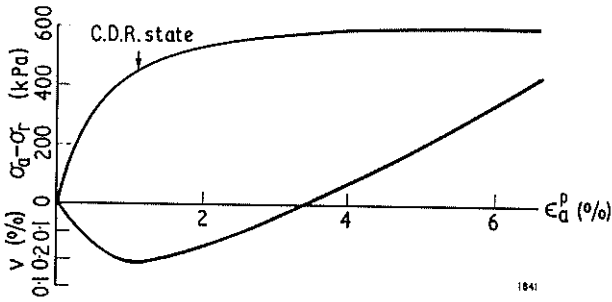


Fig. 4 Typical plastic response of the sand subjected to Series A test

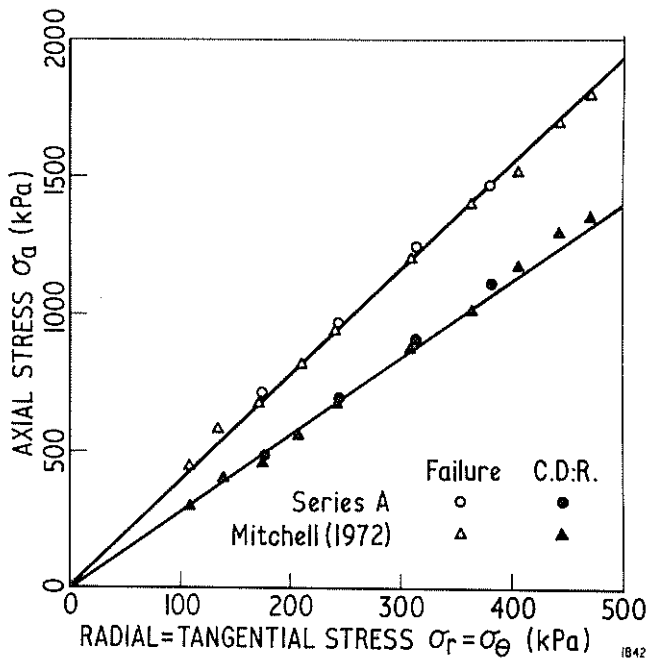


Fig 5 Failure and C.D.R. stress conditions for equal minor principal stresses ( $\sigma_r = \sigma_\theta$ )

stress-strain behaviour of the material and the boundary conditions. The boundary stresses and strains can be measured accurately and this is used to verify a three-dimensional, predictive, model. The stresses and strains can, however, be approximately determined by assuming a linear distribution through the sample, so that a theory can be formulated.

The volumetric change response of the material, when subjected to Series A and B tests, exhibited a similar type of behaviour (e.g. Fig. 2,3). The sand contracts initially until a certain stress state is reached after which the sand grains ride over each other and the material, as a whole, expands. This stress state is referred to as the contraction to dilation reversal (C.D.R.) stress condition which is an important material property, since excessive strains do not occur before this stress state is reached and yet it occurs at a load carrying capacity of about 75% of the failure load capacity.

#### 4 ANALYSIS OF RESULTS

As stated in the Introduction, the elastic (recoverable) strains were identified and subtracted from the total behaviour to leave the plastic strains (see Fig. 4). These were analysed using classical plasticity theory the three components of which were formulated separately.

##### (a) Work-hardening Law

As void ratio can be expressed in terms of volumetric strain then a plastic volumetric strain-stress

relationship, if determined, will define work hardening. From Fig. 4 it is obvious that the plastic volumetric change behaviour is bounded by the C.D.R. and failure stress states: therefore these states must be defined in a three dimensional stress space. Using the Series A test results and other results from Mitchell (Ref. 8), the failure and C.D.R. states followed the relationship  $\sigma_d/(\sigma_r = \sigma_\theta) = 3.60$  ( $\phi = 34^\circ$ ) and  $\sigma_d/(\sigma_r = \sigma_\theta) = 2.78$  ( $\phi = 28^\circ$ ) respectively (see Fig. 5).

Using the Series B test results the C.D.R. and failure state was reduced to a  $\sigma_p = 1$  kPa stress plane as shown in Fig. 6. The results indicate that the extended Von-Mises criterion fits the results better than the Mohr-Coulomb or Tresca criterion. This can be mathematically expressed as

$$\text{C.D.R. stress state } \frac{\sigma_q}{\sigma_p} = 0.527 \quad (2)$$

$$\text{failure stress state } \frac{\sigma_q}{\sigma_p} = 0.657 \quad (3)$$

These relationships were found to be material constants independent of stress history and are limiting conditions of the material.

The plastic volume change-stress behaviour can now be analysed in two regions, namely between the stress origin and the C.D.R. state, and between the C.D.R. and failure stress state. In the first region the volumetric strains from Series A and B tests were plotted against the hydrostatic stress, and the linear relationship

$$v_p = 2.2 \times 10^{-6} \sigma_p \quad (4)$$

was found to fit the results approximately (see Fig. 7, Series A shown only). As these strains are very small at low stress values, the readings could not be accurately measured; however the trend of behaviour is still clearly evident.

In the stress region between the C.D.R. and failure state a common relationship was found for all tests (see Fig. 8, Series B shown only).

$$\text{i.e. } v_p = 2.2 \times 10^{-6} \sigma_p + \left\{ \ln \left[ \frac{0.657 - \sigma_q/\sigma_p}{0.13} \right] \right\} / 350 \quad (5)$$

This equation approaches infinity at failure which is not, of course, experimentally true but very large volumetric changes do occur for a very small change in stress at the failure state. These two equations (4 and 5) represent an experimentally derived work-hardening property for the plastic response of the material in three dimensions.

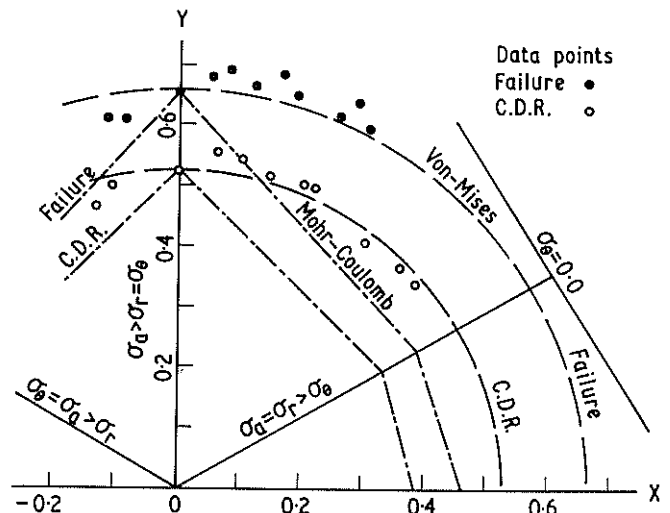


Fig. 6 Failure and C.D.R. stress conditions on a reduced deviatoric stress plane for  $\sigma_p$  equal to unity

(b) Plastic Potentials

As stated in eq. 1, the components of the plastic strain increments  $d\epsilon_{ij}^p$  may be found by partially differentiating  $g(\sigma_{ij})$  with respect to  $\sigma_{ij}$ . The conclusion can be drawn from this that only the differential or the slope of the plastic potential has to be determined. This will yield the ratio of the desired strain components and as the sum of the strains is specified by work hardening, this should be quite sufficient. Fig. 9 demonstrates how this slope can be determined for the  $\sigma_q > \sigma_p = \sigma_\theta$  stress condition. The stress and plastic strain increments are calculated in terms

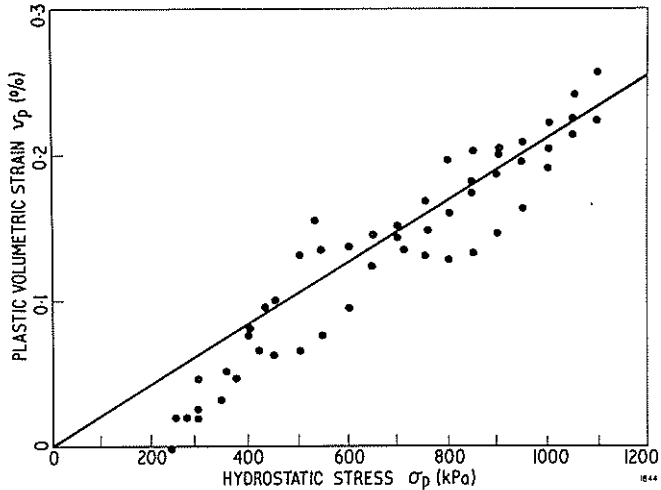


Fig. 7 Plastic volumetric strain variation up to C.D.R. state

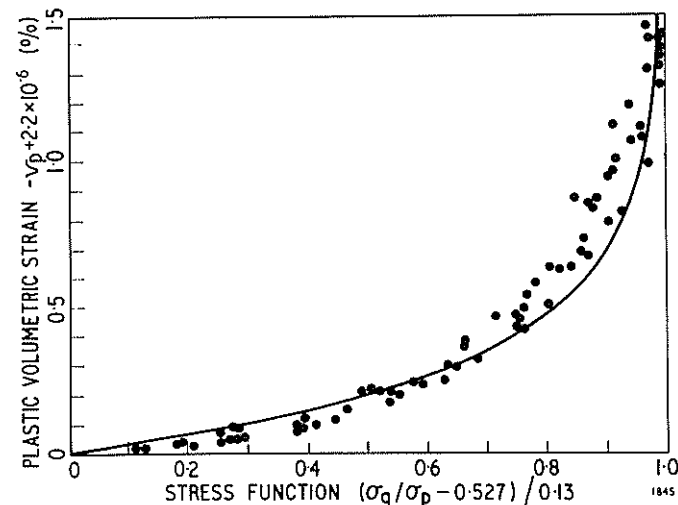


Fig. 8 Plastic volumetric strain after C.D.R. state

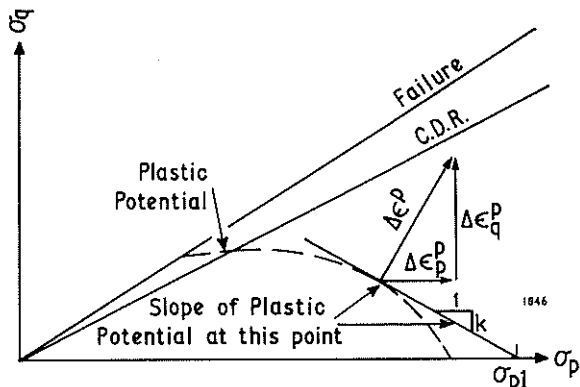


Fig. 9 Plastic potential plot  $\sigma_p - \sigma_q$  stress plane

of the deviatoric and hydrostatic components and then plotted on this stress plane. It is observed that the slope at any stress point is  $\Delta\epsilon_p^p / \Delta\epsilon_q^p$  calculated for the same stress point. Thus the plastic potential can be considered as a straight line passing through the value of  $\sigma_{p1}$  on the  $\sigma_p$  axis. The equation of this line is

$$\sigma_q = K(\sigma_{p1} - \sigma_p) \tag{6}$$

$$\text{where } K = \Delta\epsilon_p^p / \Delta\epsilon_q^p$$

Hence the equation of the plastic potential at this point is

$$g(\sigma_{ij}) = \sigma_q + K(\sigma_q - \sigma_{p1}) \tag{7}$$

If the expression is differentiated with respect to any stress variable then  $\sigma_{p1}$  will disappear from the equation.

To calculate the slope at a particular stress point in space experimentally it is necessary to subject a sample to that stress state, apply a small increment in stress and then measure the small plastic strain changes. This is virtually impossible to perform, so an alternative approach was used. The material behaviour was approximated mathematically using a non-linear bulk and shear modulus method of analysis. This could only be done in the contractive stress zone (i.e. up to C.D.R. stress state) as a prerequisite of the method is that no volume change occurs under the influence of shear stress alone. It was found that the closest agreement was achieved with two different values of both bulk and shear modulus, the average of them giving a good agreement. The plastic potential slopes were calculated for both and the average taken as the correct value.

Fig. 10. demonstrates this and the fact that the slopes are proportional to the stress ratio  $\sigma_q/\sigma_p$  in the form

$$K = 0.55 \exp \frac{\sigma_q/\sigma_p}{0.207} - 0.03 \tag{8}$$

If this value of  $K$  is inserted into eq. 7, then the plastic potentials are defined in the  $\sigma_p = \sigma_\theta$  stress plane below the C.D.R. state.

At the C.D.R. state the plastic volumetric change increment of the material is equal to zero; hence at this stress state  $\Delta\epsilon_p^p$  is equal to zero and so the slope of the plastic potential is zero, i.e. parallel to the  $\sigma_p$  axis. After the C.D.R. stress state the sample is plastically dilating, i.e.  $\Delta\epsilon_p^p$  is negative and the slope of the plastic potential

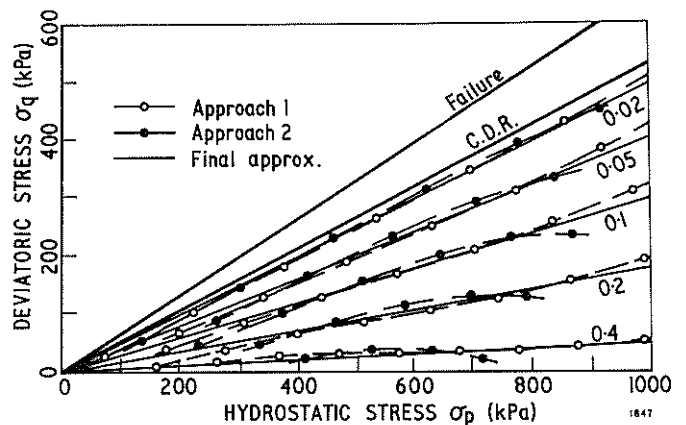


Fig. 10 Contours of plastic potential gradients up to C.D.R. stress state

is also negative. Various values of the slope were tried in this region and it was found empirically that a constant value of

$$K = -0.115 \quad (9)$$

gave most accurate results.

It is now possible to calculate the plastic stress for a known stress. Referring to eqs. 1 and 7, it follows that

$$\Delta \epsilon_{\alpha}^p = \frac{\lambda d[\sigma_q + K(\sigma_p - \sigma_{p1})]}{d\sigma_{\alpha}} \quad (10)$$

if  $\sigma_p$  and  $\sigma_q$  are expanded this equation can be expressed as

$$\Delta \epsilon_{\alpha}^p = \frac{\lambda K}{\sqrt{3}} \left( \frac{2\sigma_{\alpha} - \sigma_r - \sigma_{\theta}}{\sqrt{3} \sigma_q K} + 1 \right) \quad (11)$$

Similarly  $\Delta \epsilon_r^p$  and  $\Delta \epsilon_{\theta}^p$  can be expressed by substituting corresponding stresses. If they are then added

$$\Delta \epsilon_{\alpha}^p + \Delta \epsilon_r^p + \Delta \epsilon_{\theta}^p = \Delta v_p = \frac{3\lambda K}{3} \quad (12)$$

However, eq. 4 and 5 define the plastic volumetric strain and consequently the incremental value  $\Delta v_p$  can be evaluated if the stress increment is known, therefore the value of  $\lambda$  is redundant and the plastic stresses are defined as

$$\Delta \epsilon_{\alpha}^p = \left( \frac{2\sigma_{\alpha} - \sigma_r - \sigma_{\theta}}{\sqrt{3} \sigma_q K} + 1 \right) \frac{\Delta v_p}{3} \quad (13)$$

similarly for  $\Delta \epsilon_r^p$  and  $\Delta \epsilon_{\theta}^p$

A special condition is when  $\sigma_q$  equals zero (i.e.  $\sigma_{\alpha} = \sigma_r = \sigma_{\theta}$ ) where eq. 13 is invalid and must be replaced by

$$\Delta \epsilon_{\alpha}^p = \Delta \epsilon_r^p = \Delta \epsilon_{\theta}^p = \frac{\Delta v_p}{3} \quad (14)$$

Due to the non-linear behaviour of the stress and strain distributions in the hollow cylinder sample the sample was mathematically analysed for the true three-dimensional loading application assuming the plastic potentials are circular about the  $\sigma_p$  axis (Ref. 7,9) i.e. they are dependent on the ratio  $\sigma_q/\sigma_p$  only. The method and results will be explained in the next section.

### (c) Yield Surface

On close inspection of eq. 4 and 13, it is realised that if a sample is loaded along a stress path such that  $\sigma_p$  remains constant then no plastic strain will occur up to the C.D.R. stress state. This implies that the material is not yielding and the stress path must therefore be within or on a yield surface. From this it seems reasonable that yield surfaces are defined as a plane of constant  $\sigma_p$ , the value of which is defined as the maximum hydrostatic stress experienced by the particular stress path being followed (Ref. 7). A number of tests were undertaken to verify the validity of this assumption. No satisfactory result was obtained and no other yield criterion became apparent. Time did not permit extensive research into this problem. Using a similar logic, a yield function after the C.D.R. stress state would be defined by the stress ratio  $\sigma_q/\sigma_p$  (see eq. 5); however this was not verified.

## 5 DISCUSSION OF RESULTS AND ANALYSIS

The stress-strain equations derived were applied to the stress paths followed by experiments. For the two-dimensional stress situation ( $\sigma_{\alpha} > \sigma_r = \sigma_{\theta}$ ) the results are good (see Fig. 11), the discrepancies

at initial loading are due to the settling down of the sample.

For the three-dimensional stress situation it was decided to calculate the change in boundary conditions of the hollow cylinder sample with change in load (i.e. vertical deformation, bore volume change and cell volume change). This was achieved by two methods.

### (a) Simple Approach

The stress and strains were assumed to be constant through the sample wall thickness, and the boundary conditions were then calculated.

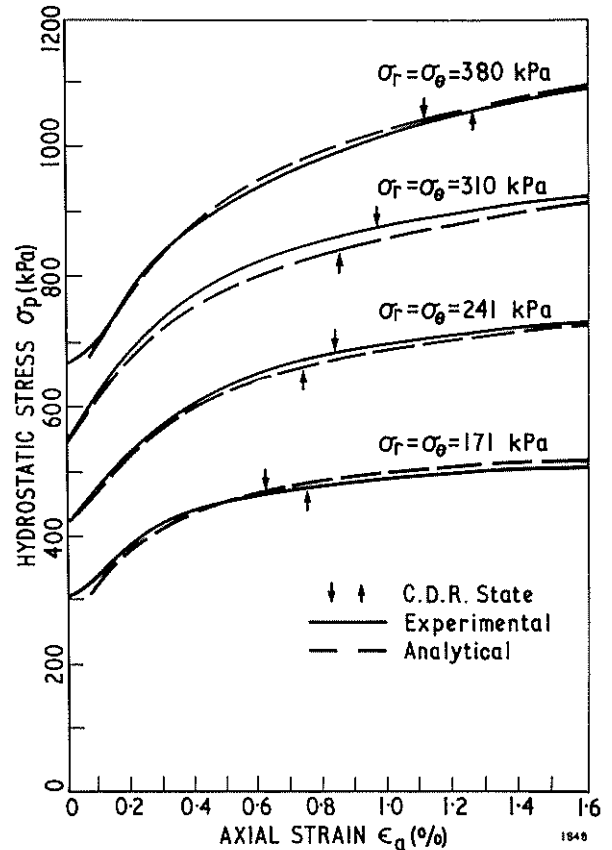


Fig. 11 Comparison of analytical and experimental data for  $\sigma_r = \sigma_{\theta}$  stress plane

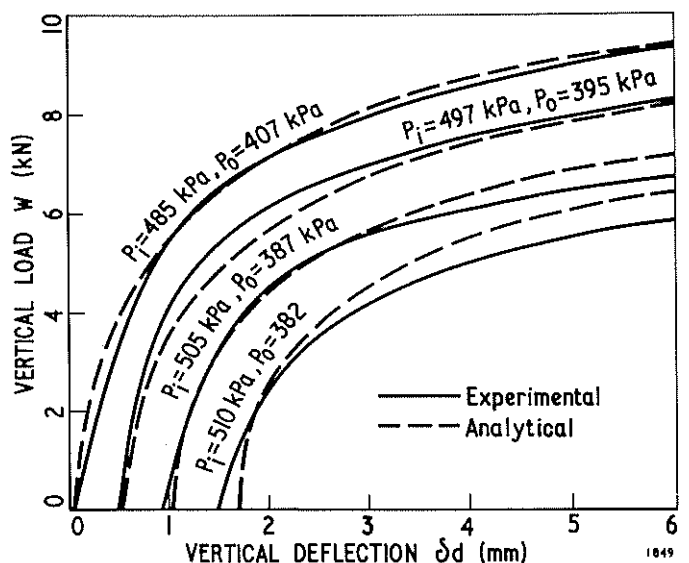


Fig. 12 Load deflection behaviour for  $P_i > P_o$  with average pressure = 445 kPa

## (b) Rigorous Solution

The sample wall was divided into ten increments from the inner face (at pressure  $P_i$ ) to the outer face (at pressure  $P_o$ ). An iterative procedure was used to completely solve all the principal stresses and strains at each node for each loading condition considered. This yielded some interesting results for the stress and strain distributions in a hollow cylinder sample (Ref. 10).

Both solutions gave very similar results for the boundary conditions. Good agreement was found between the analytically derived and experimental behaviour of the material for the load situation where the internal pressure is greater than the external pressure ( $\sigma_a > \sigma_r > \sigma_\theta$ ) as shown in Fig. 12. The agreement was not as good for the loading case  $P_o > P_i$  with discrepancies occurring up to fifty percent.

## 6 CONCLUSIONS

Using a hollow cylinder apparatus, an elastic work-hardening plastic solution for a sand at a constant initial void ratio has been developed for three-dimensional stress space. To the author's knowledge, this is the first work undertaken to use an elasto-plastic model incorporating elastic theory and classical plasticity theory in its entirety. This approach has been shown to be a satisfactory soil model in the three-dimensional stress situation for a simple stress path but does not allow for complex loading paths, since the yield surface is not completely defined. A complete method is given to generate the solution. The main characteristics of the plastic behaviour are:

- a. the plastic volumetric strain up to the C.D.R. stress state is linearly dependent on the hydrostatic stress;
- b. plastic potentials can be totally defined by the ratio of the deviatoric stress over the hydrostatic stress;
- c. the C.D.R. and failure state follow a Von Mises-type distribution;
- d. the C.D.R. stress state is a better design criterion than the failure state as only limited strains occur before the stress state is reached, and it is easier to determine than the failure state;
- e. the standard triaxial test can be used instead of the more complicated hollow cylinder test, because the results obtained from equal, minor principal stresses are sufficient to derive the analytical model;
- f. the mathematical model found for the stress-strain behaviour in the three-dimensional stress field is suitable for current computer methods.

## 7 ACKNOWLEDGEMENTS

The investigation on which this paper is based was undertaken by the author in partial fulfillment of the requirements for the degree of Master of Engineering at the University of Adelaide.

Acknowledgement is made to Dr. M. Arnold and the staff of the Civil Engineering Department of the University of Adelaide.

## 8 REFERENCES

1. GREEN, G.E. Correspondence on: A New Soil Testing Apparatus. Geotechnique, Vol. 17, No. 3, 1967, p. 295.
2. MAHKLOUF, H.M. and STEWART, J.J. Factors Influencing the Modulus of Elasticity of Dry Sand. Proc. 6th Int. Conf. on Soil Mech. & Found. Engng., 1965, Vol. 2, pp. 298-302.
3. HOLUBEC, I. Elastic Behaviour of Cohesionless Soil. Soil Mech. & Found. Div., A.S.C.E., Nov. 1968, Vol. 94, No. SM6, p. 1215.
4. EL-SOHBY, M.A. and ANDRAWES, K.Z. Deformation Characteristics of Granular Material Under Hydrostatic Compression. Canad. Geotechn. J., 1972, Vol. 9, pp. 338-350.
5. HILL, R. The Mathematical Theory of Plasticity. Oxford Uni. Press, London, 1950.
6. POOROOSHASB, M.B., HOLUBEC, I. and SHERBOURNE, A.N. Yielding and Flow of Sand in Triaxial Compression, Part 1: Canad. Geotechn. J., Nov. 1966, Vol. 3, No. 4. Parts 2, 3: Canad. Geotechn. J., 1967, Vol. 4, No. 4.
7. ARNOLD, M. and MITCHELL, P.W. Sand Deformation in Three-Dimensional Stress State. Proc. 8th Int. Conf. Soil Mech. & Fdn Engng., 1973, Vol. 1, pp. 11-18.
8. MITCHELL, P.W. Behaviour of Sand under Three-Dimensional Stress States, M.E. Thesis, 1972, University of Adelaide.
9. ROSCOE, K.H., SCHOLFIELD, A.M. and THURAIRAJAH, A. Yielding of Clays in States Wetter than Critical. Geotechnique, 1962, Vol. 13, No. 3, pp. 211-240.
10. PAPPIN, J.W. 3-D Elastic-plastic Analysis of Sand. Submitted as M.E. Thesis, 1974, University of Adelaide.